CHEMISTRY
A EUROPEAN JOURNAL

DOI: 10.1002/chem.200601901

Ring-Borylated 15-Electron and 17-Electron *ansa*-Chromocene Complexes, their Physical Properties and Molecular Structures

Pamela J. Shapiro,*[a] Piet-Jan Sinnema,[a] Philippe Perrotin,[a] Peter H. M. Budzelaar,[b] Høgni Weihe,[c] Brendan Twamley,[a] Ralph A. Zehnder,[a] and Justin J. Nairn[a]

Abstract: A detailed study of the thermal decomposition of the zwitterionic, ring-borylated *ansa*-chromocene hydrido carbonyl complex [Cr(CO)H-{$Me_4C_2(C_5H_4)[C_5H_3B(C_6F_5)_3]$}] (**2**) is described. This complex is formed in the reaction between [Cr(CO){Me_4C_2-$(C_5H_4)_2$}] (**1**) and $B(C_6F_5)_3$ in toluene at −78 °C. Above −25 °C, **2** decomposes to a 50:50 mixture of the low-spin, 17e Cr^{III} complexes [Cr(CO){$Me_4C_2(C_5H_4)$-$[C_5H_3B(C_6F_5)_3]$}] (**3b**) and [Cr(CO)-{$Me_4C_2(C_5H_4)_2$}][$HB(C_6F_5)_3$] (**4**). Carbon monoxide elimination from **3b** generates high-spin, 15e [Cr{Me_4C_2-$(C_5H_4)[C_5H_3B(C_6F_5)_3]$}] (**3a**), which coordinates two other electron-donating ligands, such as xylyl isocyanide, PMe_3, and PPh_2Me to form the low-spin, 17e electron complexes **3c**, **3d**, and **3e**, respectively. High-spin, 15e [Cr{Me_4C_2-$(C_5H_4)_2$}][$HB(C_6F_5)_3$] (**5**) is generated by heating **3b** in toluene at 100 °C and periodically removing the evolved CO. Efforts to isolate more than a few X-ray quality crystals of **5** were thwarted by its tendency to form an insoluble precipitate (**6**) with the same molecular formula. Heating the solution of **5** at 120 °C results in its partial conversion (ca. 28%) to **3a**, thereby allowing the formation of **3a** in yields as high as 74% from the reaction between **1** and $B(C_6F_5)_3$. The X-ray crystal structures of **3b–e** and **5** are described. Cyclic voltammetry measurements on **3a–e** reveal a dramatic reduction in the redox potentials of the complexes relative to their non-borylated analogues. DFT calculations show that this is due primarily to electrostatic stabilization of the oxidized species by the negatively charged borylate group. EPR and ^{19}F NMR spectroscopy allow **3a** to be distinguished from its Lewis base adducts **3b–e** and reveal the relative affinities of different Lewis bases for the chromium.

Keywords: chromocene · cyclic voltammetry · density functional calculations · EPR spectroscopy · zwitterions

Introduction

Bent-metallocene complexes of the early transition metals and lanthanide metals of Groups 3–6 have contributed substantially to our understanding of bonding and reactivity in organometallic systems and have been responsible for major breakthroughs in homogeneous catalysis, especially alkene polymerization catalysis. However, the chemistry of bent-sandwich chromocene has largely eluded examination. This situation is most likely due to the lability of the cyclopentadienyl rings on high-spin, 16e parallel-ring chromocenes[1,2] and the relatively high spin-pairing energy penalty involved in forming an electronically saturated bent sandwich derivative such as $[Cr(CO)Cp_2]$.[3,4] The strategy that we have pursued to gain access to the chemistry of bent chromocene has been to employ a bridged dicyclopentadienyl ligand framework to enforce a bent geometry between the cyclopentadienyl rings on chromium. The effectiveness of this approach was initially demonstrated by Brintzinger and coworkers, who reported the first *ansa*-chromocene complex, [Cr(CO){$Me_4C_2(C_5H_4)_2$}] (**1**), in 1983.[5] Unlike $[Cr(CO)Cp_2]$, complex **1** is stable in the absence of a CO atmosphere. In fact, the CO ligand is *required* to stabilize the 16e *ansa*-chromocene fragment. Improved synthetic routes to **1** and related isocyanide derivatives[6–8] have allowed

[a] Prof. P. J. Shapiro, Dr. P.-J. Sinnema, P. Perrotin, Dr. B. Twamley, Dr. R. A. Zehnder, J. J. Nairn
Department of Chemistry, University of Idaho
Moscow, Idaho, 83844–2343 (USA)
Fax: (+1) 208-885-6173
E-mail: shapiro@uidaho.edu

[b] Prof. P. H. M. Budzelaar
Department of Chemistry, University of Manitoba
Winnipeg, Manitoba, R3T 2N2 (Canada)

[c] Prof. H. Weihe
Department of Chemistry, University of Copenhagen
Universitetsparken 5, 2100, Copenhagen (Denmark)

Supporting information for this article is available on the WWW under http://www.chemeurj.org/ or from the author.

these complexes to be used as a basis for exploring bent-chromocene reactivity.

Previously we reported that the electrophilic addition of $B(C_6F_5)_3$ to **1** in toluene yields 18e diamagnetic [Cr(CO)H{$Me_4C(C_5H_4)[C_5H_3B(C_6F_5)_3]$}] (**2**), the first structurally characterized Cr^{IV} bent-metallocene species.[9] Above −20°C, **2** decomposes cleanly to a 1:1 mixture of two Cr^{III} species, low-spin 17e [Cr(CO){$Me_4C_2(C_5H_4)[C_5H_3B(C_6F_5)_3]$}] (**3b**) and low-spin 17e [Cr(CO){$Me_4C_2(C_5H_4)_2$}][$HB(C_6F_5)_3$] (**4**) (Scheme 1). Here we present the molecular structures, physical properties, and reactivity of these complexes and other 15e and 17e species that are derived from them. From a combination of X-ray crystallography, cyclic voltammetry, EPR, and ^{19}F NMR studies we have found that the $-B(C_6F_5)_3$ substituent has interesting and useful effects on the redox properties, reactivity, and stability of the *ansa*-chromocene complexes that could be extended to other *ansa*-metallocene systems. DFT calculations on model complexes offer some insight into these effects.

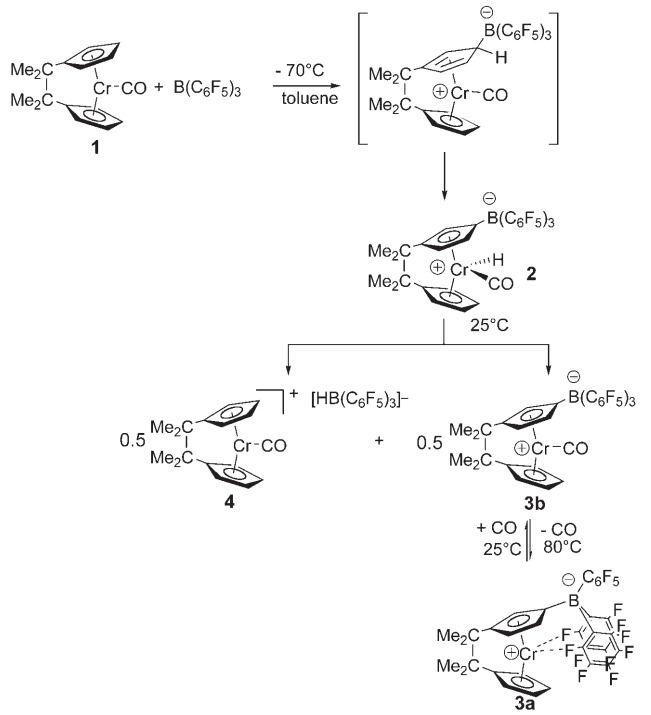

Scheme 1. Products of the reaction between **1** and $B(C_6F_5)_3$ as a function of temperature.

Results and Discussion

Isolation and identification of products from the thermal decomposition of [Cr(CO)H{$Me_4C_2(C_5H_4)[C_5H_3B(C_6F_5)_3]$}] (2): The reaction between red-brown [Cr(CO){$Me_4C_2(C_5H_4)_2$}] (**1**) and $B(C_6F_5)_3$ occurs immediately in [D_8]toluene at −78°C, forming diamagnetic, orange-brown **2**. This complex is stable indefinitely below −20°C, but decomposes above this temperature to form paramagnetic products. Decomposition of a solution sample of **2** in toluene at room temperature is complete within 12 h. The resulting dark brown solution yields very little free CO at this stage (0.02–0.03 mol CO per mol Cr was collected with a Toepler pump). Heating the mixture at 35–40°C produces a deep green solution along with an orange crystalline precipitate after approximately 2 h. The evolution of CO by the heated mixture was monitored with a Toepler pump until no further CO was produced (ca. 22 h), giving a yield of 0.49 mol CO per mol Cr. The dark green solution afforded crystals of the zwitterionic, 15e ring-borylated compound [Cr{$Me_4C_2(C_5H_4)[C_5H_3B(C_6F_5)_3]$}] (**3a**). The orange crystalline precipitate was identified as 17e [Cr(CO){$Me_4C_2(C_5H_4)_2$}][$HB(C_6F_5)_3$] (**4**) (Scheme 1).

An equilibrium between green **3a** and its red-brown 17e carbonyl derivative [$Me_4C_2(C_5H_4)${$C_5H_3B(C_6F_5)_3$}]Cr(CO) (**3b**) was evident from the fact that less CO was isolated from the thermal decomposition of **2** if free CO was not periodically removed from the vessel. Furthermore, drops of the dark green solution that deposited on cooler regions of the vessel wall changed to orange-brown. The same color change was observed at the surface of the solution when it was cooled in liquid nitrogen. Exposure of a dark green solution of **3a** in benzene to an atmosphere of CO produced an immediate color change to brown. Application of a dynamic vacuum to the solution caused the color to revert back to green. These color changes were accompanied by a change in the magnetic susceptibility of the sample, as determined by using Evans' solution NMR method.[10]

Compound **3b** was isolated in 81% yield as a red-brown, crystalline complex by applying a CO atmosphere to a solution of **3a** in benzene layered with pentane. Magnetic susceptibility measurements on **3a** and **3b** as solids gave magnetic moments of 3.8 and 1.8 μ_B, respectively, showing that coordination of CO by chromium leads to a change in the spin of the complex from $S=3/2$ to $S=1/2$. Ionic complex **4** is also low spin, with $\mu_{eff}=2.0\ \mu_B$. The CO stretching vibration of **3b** (1978 cm^{-1}) is slightly lower in energy than that of complex **4** (1989 cm^{-1}). The molecular structures of complexes **2** and **3a** were described previously.[9] The molecular structure of **3b** is shown in Figure 1. Selected structural parameters for the complex are listed in the caption for Figure 1 and in Table 1.

An especially interesting feature of the structure is the presence of a π-stacking interaction between the carbonyl ligand on chromium and one of the pentafluorophenyl rings of the boryl substituent. Whereas π-stacking interactions between arene rings are common,[11–14] to our knowledge this is the first example of a π-stacking interaction between an arene ring and a carbonyl ligand. Similar π-stacking interactions have been described between one of the pentafluorophenyl rings and the xylyl isocyanide ligand (CNxyl) of [Cr(CNxyl){$Me_4C_2(C_5H_4)[C_5H_3B(C_6F_5)_3]$}] (**3c**)[9] and [Cr(CNxyl)CN{$Me_4C_2(C_5H_4)[C_5H_3B(C_6F_5)_3]$}].[15] The distance between the center of the C18–C23 ring plane ring

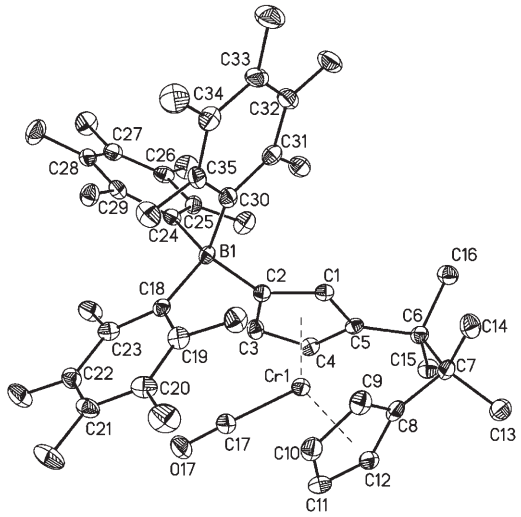

Figure 1. Thermal ellipsoid drawing (30%) of **3b**. Hydrogen atoms and fluorine labels have been omitted for clarity. Selected bond lengths (Å) and angles (°): Cr–CO 1.871(3), CrC–O 1.147(5), B1–C2 1.626(6), Cr–centroid(C1–C5) 1.82, Cr–centroid(C8–C12) 1.82; centroid-C2-B1 173.2, Cr1-C17-O17 178.5.

along its normal and the C17–O17 bond is 3.15 Å as compared with interplanar distances of 3.4–4.4 Å for fluoroaryl–aryl stacking interactions.[11–14] The dihedral angle between the cyclopentadienyl rings planes of **3b** is significantly wider than that of **3a** and slightly narrower than that of **2** (Table 2). Thus, increasing the number of ligands in the equatorial wedge causes the cyclopentadienyl rings to tilt back more on the metal. The Cr–centroid distances are similar for both cyclopentadienyl rings, so there is no noticeable strain imposed by the bulky boryl group on the cyclopentadienyl–chromium interaction. The boron deviates slightly from the plane of the attached cyclopentadienyl ring with a centroid-C2-B1 angle of 173.2°.

The molecular structure of **4** is similar to $[Cr(CO)\{Me_4C_2(C_5H_4)_2\}][B(C_6F_5)_4]$, which was reported in an previous communication.[16] Selected structural parameters for the complex are listed in Table 1 and crystallographic data is listed in Table 2.

When the products of the reaction between **1** and $B(C_6F_5)_3$ in toluene were heated at a higher temperature (100–105 °C) over a longer time (40–50 h) with periodic removal of free CO from the vessel, 0.97 mol CO per mol Cr was collected. Passage of the gas over a heated column of CuO yielded only CO_2, confirming that the gas consisted exclusively of CO. The thermolysis product consisted of **3a**, which was isolated in 47% yield, and a brown-yellow, insoluble solid (**6**) that was isolated in 43% yield. An IR spectrum of **6** showed a B–H stretch at 2376 cm^{-1} and other features consistent with a $[HB(C_6F_5)_3]^-$ counterion, but it did not exhibit a CO stretch. The insolubility of **6** in a variety of solvents (e.g. THF and CH_2Cl_2) precluded its further structural characterization. The elemental analysis (C, H) of **6** was consistent with the molecular formula for $[Cr\{Me_4C_2(C_5H_4)_2\}][HB(C_6F_5)_3]$, the CO elimination product of **4**. The material exhibited a magnetic moment of 3.8 μ_B at room temperature, consistent with three unpaired electrons on chromium. The formation of **6** is irreversible. It remained insoluble in THF when exposed to an atmosphere of CO.

To confirm that **6** originated from **4**, the thermolysis of **4** alone was examined. On being heated at 90–100 °C, the clear yellow-orange solution of **4** in toluene turned dark green over the course of 30 min. After approximately 4 h and three gas collections at one hour intervals, 0.98 mol of CO gas per mol Cr was collected. The resulting dark green solution contained some yellow precipitate, which was confirmed by IR analysis to be **6**. As the solution was concentrated under vacuum, more yellow precipitate formed.

Although we were unable to isolate substantial amounts of the soluble green compound, we were able to obtain some dark green crystals suitable for X-ray analysis. The dark green material was identified as $[Cr\{Me_4C_2(C_5H_4)_2\}][HB(C_6F_5)_3]$ (**5**) (Scheme 2). Its molecular structure is shown in Figure 2. Selected structural parameters are listed in the figure caption and in Table 1.

Interestingly, heating a solution of **4** in toluene at even higher temperature (120–125 °C) produced not only **6** (55% yield), but **3a** as well (28% yield), along with 0.90 equiv of CO and 0.35 equiv of H_2. Apparently the hydroborate anion transfers its hydride back to chromium, generating a neutral *ansa*-chromocene hydride intermediate and $B(C_6F_5)_3$. Subsequent electrophilic addition of the $B(C_6F_5)_3$ to the cyclopentadienyl ring of the *ansa*-chromocene hydride intermediate must then occur to generate **3a** and H_2. However, when the thermolysis of **4** was conducted under 800 mm CO, neither H_2 nor **3b** were formed and only a very small amount of **6** precipitated. Therefore, only the naked 15e chromium species is able to re-abstract a hydride from $[HB(C_6F_5)_3]$, as depicted in Scheme 3.

At lower temperatures (<100 °C) only a 50% theoretical yield of **3a** is achievable from the disproportion of **2** to **3b** and **4**; however, the partial conversion of **5** to **3a** at 120 °C indicated that yields of **3a** from **2** could be increased by carrying out the thermolysis of **2** at 125 °C, while removing free

Table 1. Summary of structural and physical parameters of complexes **1**, **2**, **3a–e**, and **5**.

	1	**2**	**3a**	**3b**	**3c**	**3d**	**3e**	**4**	**5**
centroid-Cr-centroid [°]	143.3(5)	140.0(1)	149.3(3)	142.5(3)	140.0(1)	142.5(3)	nd	142.1(2)	149.4(4)
Cp < Cp xy[°]	38.5(5)	42.4(1)	36.9(2)	41.0(2)	42.4(1)	41.0(2)	nd	38.4(2)	36.4(2)
$\tilde{\nu}$ CO(CNR) [cm^{-1}]	1905	1992	na	1978	1992	na	na	1989	na
μ_{eff}[a] [μ_B]	na	na	3.8	1.8	1.8	1.9	2.0	2.0	nd

[a] From measurements on the solids. [b] na = not applicable. [c] nd = not determined.

Table 2. Crystallographic data for compounds **3b**, **3d**, **3e**, and **5**.

	3b	**3d**	**3e**	**4**	**5**
formula	$C_{35}H_{19}BCrF_{15}O$	$C_{37}H_{28}BCrF_{15}P$	$C_{42}H_{30}BF_{15}P$	$C_{35}H_{21}BCrF_{15}O$	$C_{34}H_{21}BCrF_{15}$
M_r	803.31	851.37	913.44	805.33	777.32
crystal system	orthorhombic	monoclinic	monoclinic	triclinic	triclinic
space group	$Pna2_1$	$P2_1/n$	$P2_1/c$	$P\bar{1}$	$P\bar{1}$
a [Å]	18.1437(7)	10.7559(18)	12.733(4)	10.0591(8)	11.3841(10)
b [Å]	11.8078(5)	20.690(3)	20.217(5)	11.8948(9)	12.2488(10)
c [Å]	14.3471(5)	15.520(3)	14.374(4)	14.9672(12)	12.7333(11)
α [°]	90	90	90	112.01(1)	94.154(1)
β [°]	90	93.826(4)	95.70(3)	90.94(2)	104.687(2)
γ [°]	90	90	90	105.35(2)	115.840(2)
V [Å^3]	3073.7(2)	3446.1(10)	3681.9(17)	1587.7(3)	1511.3(2)
Z	4	4	4	2	2
T [K]	203(2)	81(2)	83(2)	203(2)	83(2)
exposure time [s]	40	30	20	30	5
frames collected	1471	1471	2132	2132	2132
ρ_{calcd} [Mg m^{-3}]	1.736	1.641	1.648	1.685	1.708
μ [mm^{-1}]	0.495	0.489	0.464	0.480	0.498
$F(000)$	1604	1716	1844	806	778
crystal size [mm^3]	$0.21\times0.09\times0.05$	$0.22\times0.10\times0.05$	$0.32\times0.08\times0.04$	$0.27\times0.26\times0.09$	$0.22\times0.20\times0.05$
θ range [°]	2.06 to 27.50	1.64 to 25.00	1.61 to 25.25	1.48 to 25.25	1.89 to 25.25
index ranges	$-13\le h\le23$	$-12\le h\le12$	$-15\le h\le15$	$-12\le h\le12$	$-13\le h\le13$
	$-13\le k\le15$	$-24\le k\le21$	$-24\le k\le24$	$-14\le k\le14$	$-14\le k\le14$
	$-18\le l\le18$	$-18\le l\le11$	$-17\le l\le17$	$-17\le l\le17$	$-15\le l\le15$
reflections collected	26842	21961	48507	20009	16950
independent reflections	7048 [R(int) = 0.0777]	6074 [R(int) = 0.1162]	6670 [R(int) = 0.0659]	5735 [R(int) = 0.0248]	5467 [R(int) = 0.0386]
data/restraints/parameters	7048/1/482	6074/0/503	6670/0/547	5735/37/409	5467/122/539
GOF	1.015	0.981	1.052	1.034	1.021
$R1$[a] [$I>2\sigma(I)$]	0.0542	0.0669	0.0438	0.0664	0.0509
$wR2$[a] [$I>2\sigma(I)$]	0.0866	0.1513	0.0944	0.1723	0.1189
Largest diff. peak/hole [e Å^{-3}]	0.510/−0.340	1.290/−0.560	0.476/−0.435	1.100/−1.298	0.783/−0.426

[a] $R1=\Sigma||F_o|-|F_c||/\Sigma|F_o|$; $wR2=\{\Sigma[w(F_o^2-F_c^2)^2]/\Sigma[w(F_o^2)^2]\}^{1/2}$.

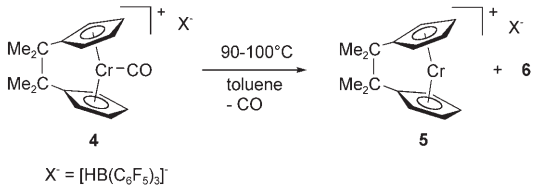

Scheme 2. Products of CO elimination from **4** (compound **6** is an insoluble brown-yellow precipitate).

CO during the course of the reaction. Indeed, **3a** was isolated in 74% yield from the thermolysis of **2** in toluene at 125°C over three days with the periodic removal of evolved gases (Scheme 4). The only other product was **6**, which, due to its insolubility, was easily separated from the solution of **3a** by filtration. In this manner, multigram quantities of **3a** can readily be prepared.

Lewis base coordination by 3a: Complex **3a** is extremely air and moisture sensitive, but is infinitely stable under an atmosphere of nitrogen or argon and is thermally robust. It is soluble in polar solvents like diethyl ether and THF and in aromatic solvents, but is insoluble in aliphatic solvents. Its reversible coordination of CO and the accompanying transition from high to low spin prompted us to examine the effect of coordinating other Lewis bases to **3a**. Addition of CNxyl to a solution of **3a** in THF or toluene produces an immediate color change from green to red-brown from the formation of [Cr(CNxyl){$Me_4C_2(C_5H_4)$[$C_5H_3B(C_6F_5)_3$]}] (**3c**), which, like **3b**, is low spin, ($\mu_{eff}=1.8\,\mu_B$). Complex **3a** also coordinates PMe_3 and $PPhMe_2$ to form red-brown **3d** ($\mu_{eff}=1.9\,\mu_B$) and **3e** ($\mu_{eff}=2.0\,\mu_B$), respectively. The ability of **3a** to bind phosphane contrasts with the behavior of the neutral

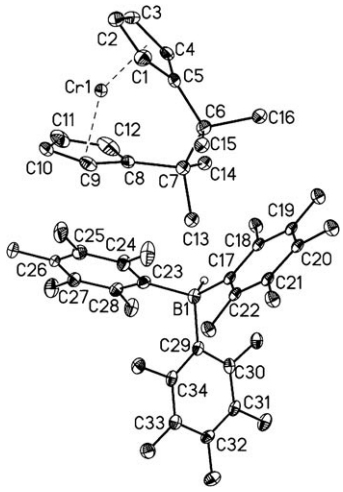

Figure 2. Thermal ellipsoid drawing (30%) of **5**. Hydrogen atoms and fluorine labels have been omitted for clarity. Selected bond distances (Å): Cr−centroid(C1–C5) 1.82, Cr−centroid(C8–C12) 1.80.

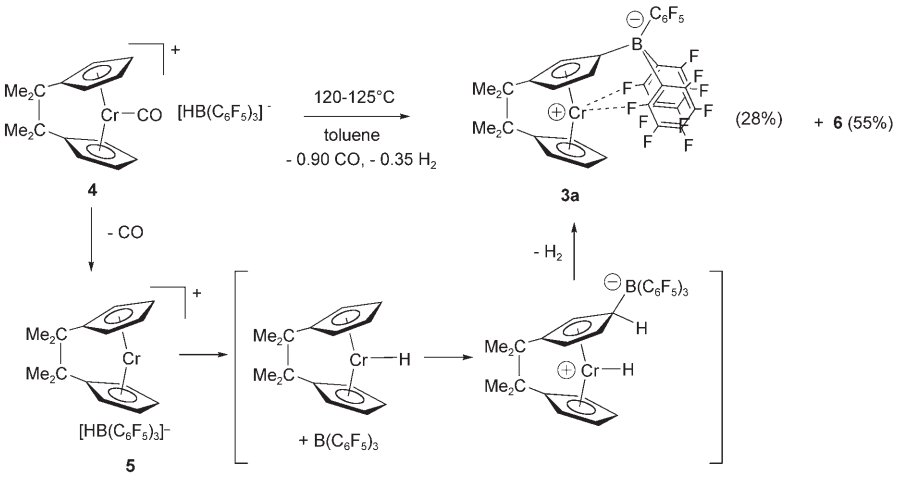

Scheme 3. Proposed mechanism for partial conversion of **5** to **3a**.

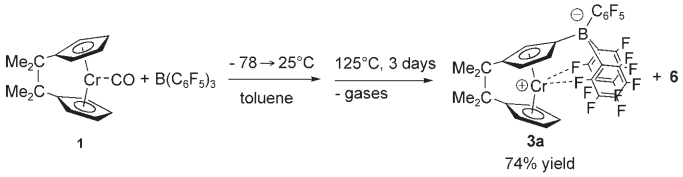

Scheme 4. One pot synthesis of **3a**.

16e *ansa*-chromocene [Cr{$Me_4C_2(C_5H_4)_2$}], which cannot be trapped with phosphanes and has so far only been shown to coordinate rod-shaped, π-accepting CO and isocyanide ligands.[17] The slightly higher magnetic moments of **3d** and **3e** relative to **3c** are probably due to the presence of **3a** as an impurity in the samples, as manifested in the EPR spectra of the complexes (vide infra).

The molecular structures of complexes **3d** and **3e** are shown in Figures 3 and 4, respectively. Crystallographic data for the complexes are listed in Table 2.

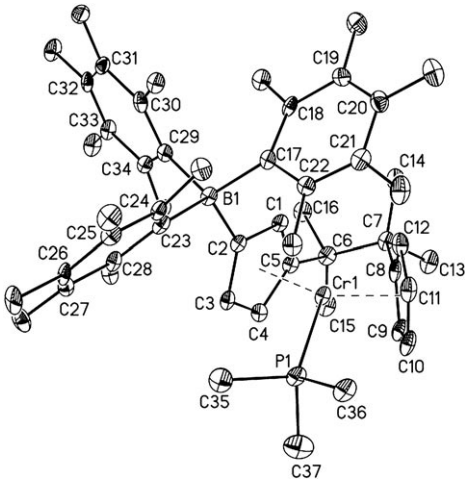

Figure 3. Thermal ellipsoid drawing (30%) of **3d**. Hydrogen atoms have been omitted and fluorine atoms unlabeled for clarity. Selected bond distances (Å): Cr–centroid(C1–C5) 1.82, Cr–centroid(C8–C12) 1.82.

NMR spectra of 3a–e: No signals are observed for the cyclopentadienyl protons and carbon atoms in ±400 ppm and ±1000 ppm windows of the ^{1}H and ^{13}C NMR spectra, respectively. This contrasts with 16e non-bridged chromocene species that do exhibit paramagnetically shifted cyclopentadienyl proton and carbon signals.[18] ^{1}H NMR signals are observed, however, for moieties more distal to the paramagnetic chromium centers in **3a–e**, such as the borylate substituent, the methyl groups of the ethanediyl

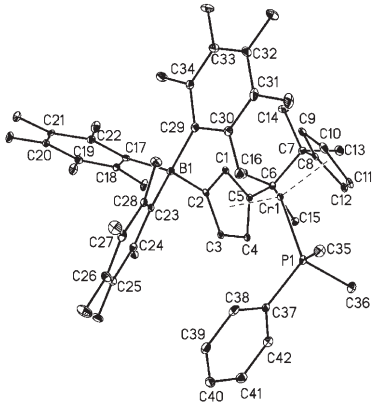

Figure 4. Thermal ellipsoid drawing (30%) of **3e**. Hydrogen atoms have been omitted and fluorine atoms are unlabeled for clarity. Selected bond distances (Å): Cr–centroid(C1–C5) 1.82, Cr–centroid(C8–C12) 1.81.

bridge, and moities attached to the phosphane and isocyanide ligands. The ^{1}H NMR spectra exhibit four broad signals (fwhh ≈500 Hz) between +1 and −11 ppm for the inequivalent methyl groups along the ethanediyl bridge. Signals for these methyl groups are not apparent in the ^{13}C NMR spectra; however, signals for the $B(C_6F_5)_3$ moieties are found in the region +140 to +240 ppm. The $B(C_6F_5)_3$ moities also exhibit two relatively sharp ^{19}F NMR signals for the *meta* and *para* fluorine atoms of the C_6F_5 groups. The *ortho* fluorine atoms are not observed, probably due to their closer proximity to the paramagnetic chromium center. There are clear differences between the ^{19}F chemical shifts of 15e, high-spin **3a** and its 17e, low-spin, Lewis base adducts. The resonances of the latter complexes are downfield (−158 to −159 ppm (*p*-F); −163 to −164 ppm (*m*-F)) of those of complex **3a** (−145 to −148 ppm (*p*-F); −153 to −156 ppm (*m*-F)). Furthermore, the separation between the signals for **3a** ($\Delta = [\delta(p\text{-F}) - \delta(m\text{-F})] = 7$–8 ppm) is larger than that for **3b–d** ($\Delta\delta = 3$–4 ppm; Figure 5). Although these ^{19}F chemical shift differences are small, indicating that there is little unpaired

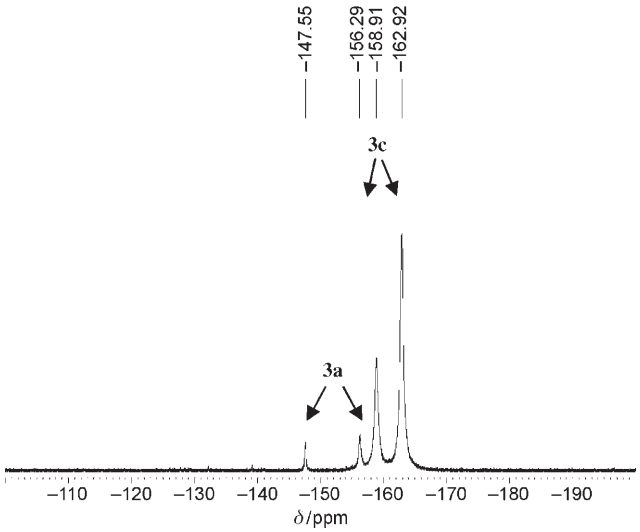

Figure 5. ^{19}F NMR spectrum of a mixture of **3a** and **3c** in [D_8]THF.

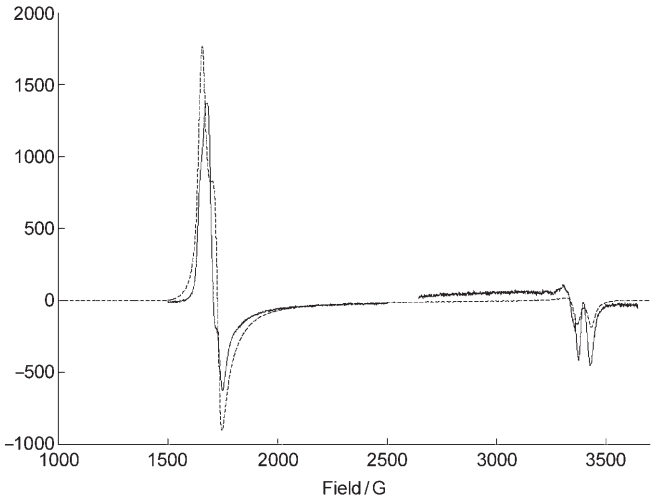

Figure 6. Solid line: Experimental EPR spectrum of a frozen THF solution of **3a** at 7 K. Dotted line: Simulated spectrum.

electron delocalization over the borate substituent, they are of sufficient magnitude to clearly distinguish high-spin 15e **3a** from its low-spin 17e Lewis base adducts (Figure 5). Hence, ^{19}F NMR spectroscopy can be used to probe the affinity of **3a** for different Lewis bases. For example, the absence of any noticeable change in the chemical shift of **3a** in the presence a large excess of either PPh_3 or pyridine indicates that **3a** has negligible affinity for these Lewis bases. This was confirmed by magnetic susceptibility measurements on the samples using Evans' solution NMR method. On the other hand, $PMePh_2$ was found to bind weakly to **3a**. Rather than exhibiting separate signals for **3a** and its $PMePh_2$ adduct, however, the variable-temperature ^{19}F NMR spectra of a mixture of **3a** and five equivalents of $PMePh_2$ in [D_8]THF exhibited only one set of *p*- and *m*-F signals that shifted with temperature. The temperature-dependent chemical shifts of these signals correlated with temperature-dependent equilibria between high-spin 15e and low-spin 17e species, as indicated by magnetic susceptibility measurements by the Evans' solution NMR method (see Supporting Information).

EPR measurements: A solution **3a** in THF was EPR-silent from 77–298 K; however, solutions of compounds **3b** and **3c** in THF displayed sharp isotropic signals with $g=2.0197$ and 2.0287, respectively, at 298 K (see Supporting Information). Compound **3d** was EPR silent at 298 K. In the presence of a 28-fold excess of PMe_3 it exhibited a broad, weak signal at $g=2.0357$ (see Supporting Information). This behavior is indicative of dynamic phosphane dissociation. Nevertheless, the ^{19}F NMR spectrum of **3d** is comparable to that of **3c**, in which the isocyanide ligand is tightly coordinated, indicating that the phosphane dissociation equilibrium lies largely toward **3d**. The low-temperature (7 K) EPR spectrum of **3a** is shown in Figure 6 along with a computer simulated spectrum. The features in the $g\approx2$ and $g\approx4$ regions are consistent with an $S=3/2$ spin system[19–21] with a large zero-field splitting. Furthermore, we tentatively assign the two equally intense lines in the $g\approx2$ region to a doublet arising from a superhyperfine interaction between the electron spin and a single coordinated F atom from a phenyl ring, rather than the two coordinated F atoms observed in the X-ray crystal structure. The features could be accounted for with the spin Hamiltonian in Equation (1) with parameter values $g=1.99$, $A_{zz}=0.006\ cm^{-1}$, $A_{xx}=A_{yy}=0.001\ cm^{-1}$, $D=5\ cm^{-1}$ and $E=0.07\ cm^{-1}$.

$$H = S_z^2 - E(S_x^2 - S_y^2) + \mu_B\, g(S_x B_x + S_y B_y + S_z B_z) + A_{xx} S_x I_x A_{yy} S_y I_y + A_{zz} S_z I_z \quad (1)$$

The magnitude of the hyperfine coupling is quite large and comparable to that of the coupling between the electron spin and the P atom of the trimethylphosphane ligand in **3d** at 7 K (Figure 7). Ti···F hyperfine coupling has also been observed in the related ring-borylated, zwitterionic titanocene complex [Ti(η^5-*i*PrC_5H_4){η^5-[1,3-*i*PrC_5H_3B(C_6F5)$_3$]}].[22]

The 7 K EPR spectrum of **3c** shown in Figure 8 is typical of an $S=1/2$ species. A sharp isotropic signal at $g=2.029$ was observed for this species at room temperature, consistent with irreversible isocyanide coordination on the EPR time scale.

Electrochemical measurements: Table 3 summarizes the electrochemical data for complexes **3a–d** (referenced to $Cp_2Fe^{0/+}$) along with data for [$CrCp_2$], **1**, and [Cr(CNxyl)-{$Me_4C_2(C_5H_4)_2$}] (**7**) for comparison. The redox potentials of the ring-borylated complexes are 400–500 mV more negative than the non-borylated complexes. The cyclic voltammogram of **3b** is more complex than the others (Figure 9). The presence of a redox couple at $E_{1/2}=-1425$ mV and a cathodic peak $E_c=-210$ mV reveal the presence of **3a** in addition to **3b** due to partial CO dissociation from the chromium in solution. A $Cr^{II/III}$ couple at $E_{1/2}=-2106$ mV is also

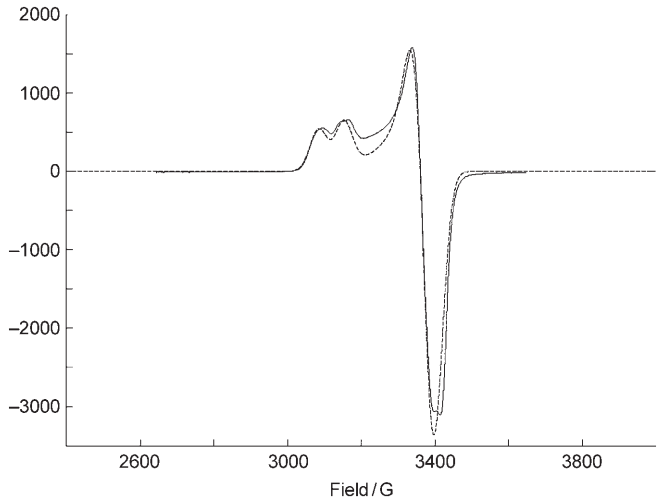

Figure 7. Solid line: Experimental EPR spectrum of a frozen THF solution of **3d** at 7 K. Dotted line: Simulated spectrum with parameters $g_x = g_y = 1.985$, $g_z = 2.15$, and phosphorus hyperfine coupling constants $A_{xx} = A_{yy} = 0.002\ cm^{-1}$, $A_{zz} = 0.006\ cm^{-1}$.

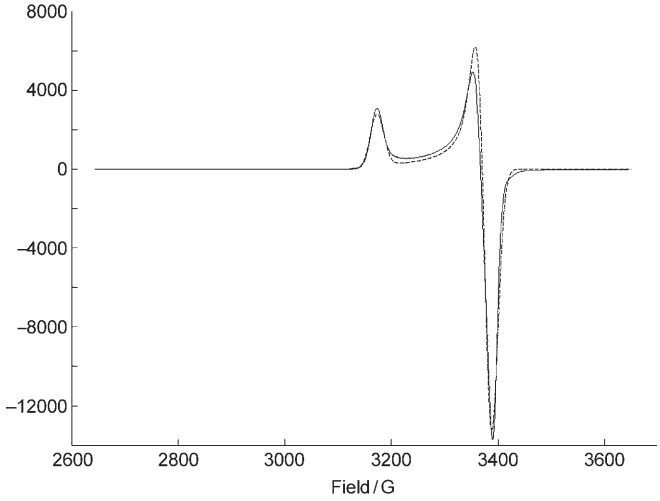

Figure 8. Solid line: Experimental EPR spectrum of a frozen THF solution of **3c** at 7 K. Dotted line: Simulated spectrum with parameters $g_x = g_y = 1.985$, $g_z = 2.115$.

evident that was not observed for **3a** and must therefore belong to **3b**. Whereas the coordination of CO by **3a** increases its redox potential, coordination of CNxyl and PMe_3 decreases it, indicating that CO acts primarily as a π acceptor in this system, while CNxyl and PMe_3 are primarily σ donors. Although **3c** exhibits a more negative $Cr^{II/III}$ redox couple than **3d**, the reverse is true for the $Cr^{III/IV}$ redox couples of these complexes.

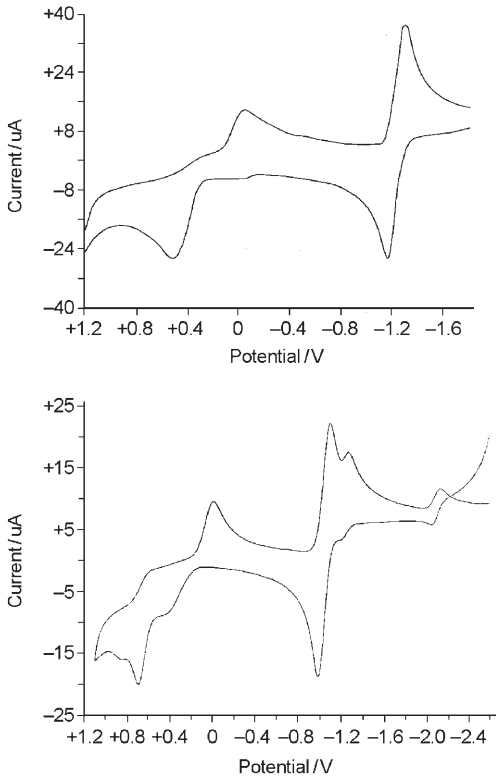

Figure 9. Cyclic voltammograms of **3a** (top) and **3b** (bottom) in THF.

DFT calculations on model 15e and 17e *ansa*-chromocene complexes: The chromocene systems $[CrCp_2]$, $[Cr\{Me_4C_2(C_5H_4)_2\}]$ and $[Cr\{Me_4C_2(C_5H_4)\}\{C_5H_4B(C_6F_5)_3\}]^-$ and their CO adducts and one-electron oxidation products were studied by DFT methods. Chromocene was used as a reference point. Geometries were optimized at the RI-bp86/SV(P) and b3-lyp/SV(P) levels. Improved single-point energies were obtained at the b3-lyp/TZVPP level and solvent corrections were calculated using the cosmo solvation model ($\varepsilon = 7.5$, THF). Frequency calculations were not feasible for the larger systems, so all energies discussed below are elec-

Table 3. Summary of cyclic voltammetry data for complexes **3a**–**d**.[a]

	Cr^{II}/Cr^{III}			Cr^{III}/Cr^{IV}			
	$(E_a+E_c)/2$ [mV]	ΔE_p [mV]	I_{ox}/I_{red}	$(E_a+E_c)/2$ [mV]	E_a [mV]	E_c [mV]	I_{ox}/I_{red}
3a	−1424	143	1.0	–	+305	−250	2.2
3b	−1244 (−1425)	220	1.0	–	+486, +276	+343, -210	–
3c	−1523	200	1.0	+24	+100	−52	1.3
3d	−1476	182	1.1	−240	−153	−326	2.8
$[CrCp_2]$[b]	−1103	94	1.0	–	–	–	–
1	−948	68	1.1	–	–	–	–
7[c]	−1181	–	–	–	–	–	–

[a] Potentials are reported relative to $[FeCp_2]^{(0/+1)}$. [b] From reference [7]. [c] From reference [8].

tronic energies. The results of the calculations are included in the Supporting Information.

The "bare" 16e metallocenes have four Cr valence electrons to distribute over three valence orbitals ($3d_{xy}$, $3d_{x^2-y^2}$, $4s+3d_{z^2}$) of very similar energies. The calculations predict the restricted closed-shell singlet ground state to be well above the lowest-lying triplet ($\Delta E_{ST}=20$–30 kcal mol^{-1}) for all systems (see Supporting Information). One might in principle expect a smooth dependence of ΔE_{ST} on the bending angle, but we find that occupations also change with bending, so no clear pattern emerges; the variation is fairly small in any case. For the 15e chromocene cations, the high-spin (quartet) state is also predicted to be lowest in energy (by 15–25 kcal mol^{-1}); again, there is no clear trend in ΔE_{DQ} as a function of bending. The effect of the borate group on the relative energies of the various spin states is also small.

The bonding in 18e chromocene–carbonyl complexes has been analyzed in detail before,[23] and will not be discussed here. The carbonyl complexes have much more stable singlet states than the 16e chromocenes. We calculate a ΔE_{ST} of around 0 at the b3-lyp level, while bp86 predicts a preference of about 10 kcal mol^{-1} for a closed-shell ground state. In view of the experimentally observed closed-shell nature of the CO complexes, the bp86 functional appears to perform best here. Again, there is no clear trend in ΔE_{ST} as a function of bending, and introduction of the borate substituent has little effect.

Bending does not appear to have a large effect on the redox potentials of the chromocenes or their CO complexes. The calculated differences at the cosmo/b3-lyp/TZVPP level are of the order of 50 mV and hence well within the error limits of the methods used. The presence of the pendant borate substituent, on the other hand, has a major impact on the oxidation potential. Inclusion of solvent effects attenuates this considerably, but the effect remains large (nearly 1 V for the *ansa*-chromocene and 0.65 V for its CO complex). In this case, the solvent corrections are so large (ca. 2 V) that errors in these values must be considerable. Nevertheless, we can conclude that the presence of a borate group stabilizes the oxidized state significantly. For the CO complex, this happens through the proximity of negative charge to the metal, rather than through any specific electronic interaction. The geometries of oxidized and reduced species do not show any discrete Cr–F interaction (shortest contact: 3.05 Å), and the insensitivity of ΔE_{ST} and CO binding strength to the presence of the borate group illustrate the electronic innocence of this substituent. For the "naked" system, of course, discrete Cr–F interactions stabilize the oxidized species, which may explain the even larger effect of the borate group.

Conclusion

The chemistry resulting from the reaction between **1** and $B(C_6F_5)_3$ is very similar to that observed by Choukroun and co-workers for the reaction between $[V(CO)Cp_2]$ and $B(C_6F_5)_3$.[24] The latter reaction produced $[VCp(C_5H_4B(C_6F_5)_3)]$, $[V(CO)_2Cp(C_5H_4B(C_6F_5)_3)]$ and $[V(CO)_2Cp_2][HB(C_6F_5)_3]$, which presumably arose from vanadium analogues of **2**, **3b** and **4**. What distinguishes the ring-borylated *ansa*-chromocene complexes described here from these and other ring-borylated early-transition-metal metallocene complexes[22,25–28] is the essential role played by the borylate group in stabilizing and affording access to *ansa*-chromocene derivatives and formal oxidation states that would have been otherwise inaccessible. This is exemplified by the dramatically different stabilities of **3a** and **5**. Whereas **3a** is stable indefinitely under a dry, nitrogen atmosphere, even when heated to 125 °C in toluene, **5** decomposes at room temperature to form insoluble **6**. Although we have no structural data to confirm this, we suspect that **6** may be a polymer resulting from the rearrangement of the dicyclopentadiene scaffold from a chelating to an intermetallic bridging arrangement.

Access to **3a** has allowed us to examine the relative affinities of different Lewis bases for the 15e cationic chromium center. Whereas NMR and EPR spectra of **3c** indicate the Cr–isocyanide interaction is strong and irreversible on the timescales of these two techniques, the phosphane adducts in **3d–f** are more labile with the following relative coordination strengths: $PMe_3 > PMe_2Ph > PMePh_2 > PPh_3$.

The substantial effect of the borylate group on the redox potentials of the chromocene complexes is not an electronic one, as presumed for a related ferrocene system.[30] Rather, it is due to the electrostatic stabilizing effect of the borylate group on increased positive charge at the metal. The existence of a significant Cr–F interaction in **3a** is supported by the above observations as well as by large superhyperfine coupling from fluorine found in the low-temperature EPR spectrum of **3a**.

Significantly, our theoretical calculations indicate that the borylate substituent has a considerably larger effect on the redox potential of the chromocene than replacing the two-carbon bridge with a single-carbon bridge, although the latter modification is predicted to increase the strength of the interaction between the metal and its CO ligand. Another very useful feature of the $B(C_6F_5)_3$ substituent is that it allows ^{19}F NMR spectroscopy to be used as a tool to distinguish between high- and low-spin 17e species and to determine the affinity of the Cr for different Lewis bases.

Experimental Section

Methods and materials: All manipulations were performed under dinitrogen, argon, or vacuum using a combination of glovebox, high-vacuum, and Schlenk techniques. HPLC grade solvents were dried by passage over alumina and then stored in line-pots, from which they were vacuum transferred from sodium/benzophenone. Argon was purified by passage over an oxy tower BASF catalyst (Aldrich) and 4A molecular sieves. Deuterated solvents were dried over 4A molecular sieves and stored in the glovebox. HPLC grade tetrahydrofuran (Fisher) was used as received for electrochemical measurements. Pyridine was dried over 4A molecular sieves. 2,6-Dimethylphenyl isocyanide (Fluka), trimethylphosphane, di-

methylphenylphosphane, methyldiphenylphosphane (Aldrich) and CO (Praxair) were used as received. $[Cr(CO)\{Me_4C_2(C_5H_4)_2\}]$ (**1**)[6] and $B(C_6F_5)_3$[30] were prepared as described in the literature.

Measurements: NMR spectra were recorded on Bruker Avance 300 MB (300 MHz ^{1}H; 75.4 MHz, ^{13}C) and Bruker Avance 500 (500 MHz ^{1}H, 125 MHz ^{13}C, 470 MHz ^{19}F, 202 MHz ^{31}P) instruments. ^{1}H and ^{13}C chemical shifts were referenced to solvent and ^{19}F and ^{13}P chemical shifts were referenced to external standards ($BF_3(OEt_2)$, $\delta = 0$ ppm; H_3PO_4(80%, aq) $\delta = 0$ ppm).

IR-spectra were obtained on a Perkin Elmer Spectrum 1000 spectrophotometer.

X-band EPR spectra (9.39 GHz) were obtained on a Bruker Biospin EMX EPR Spectrometer equipped with a liquid helium variable temperature system. Measurements were performed on 10^{-2}–10^{-3} M solutions of the complexes in THF in 4 mm quartz tubes fitted with plastic caps that were secured with parafilm.

Magnetic susceptibilities were determined on either solid samples of the complexes using a Johnson Matthey Magnetic Susceptibility Balance Type MSB, model MK I or on solutions of the samples in toluene according to Evans' NMR method.[10] Molar magnetic susceptibilities were corrected for diamagnetism using Pascal constants.[32]

Cyclic voltammetry measurements were performed on a BAS CV50W voltammetric analyzer in a nitrogen-filled glove box. Potentials were measured, without IR compensation, against a reference electrode consisting of a silver wire immersed in a solution of $AgNO_3$ (0.01 M) in acetonitrile, using a glassy carbon working electrode and a platinum wire as the counter electrode. Measurements were performed on solutions of the sample complex (< 1 mM) in THF containing 0.3 M $[NBu_4][PF_6]$ electrolyte. All potentials are referenced to the ferrocene$^{0/1+}$ couple, which was measured separately prior to each sample measurement.

H_2 and CO gases generated in the reactions were measured with a homemade Toepler pump system.[33] Speciation of the gases was accomplished by oxidizing them over an electrically heated column of copper oxide (320 °C) and collecting the oxidized species in U-shaped traps cooled at 0 °C (H_2O) and −78 °C (CO_2).

Elemental analyses were determined by Desert Analytics (Tuscon, AZ).

Calculations: DFT calculations were carried out with the Turbomole program[34,35] coupled to the PQS Baker optimizer.[36,37] Calculations on open-shell systems used the spin-unrestricted formalism. Geometries were optimized without constraints at the bp86[38,39]/RIDFT[40] level using the Turbomole SV(P) basis set[34,41] on all atoms. Improved energies were obtained from single-point calculations at the b3-lyp level[42–45] using the TZVPP basis.[34,46] Solvent corrections were calculated at the b3-lyp/TZVPP level using the COSMO solvation model[47] with a dielectric constant of 7.5 (THF). For these relatively large systems, vibrational analyses (and hence thermal corrections) were not feasible.

EPR simulations were performed with program SIM.[48]

Characterization of reaction between 1 and $B(C_6F_5)$ at 35–40 °C—Isolation of $[Cr(CO)\{Me_4C_2(C_5H_4)_2\}][HB(C_6F_5)_3]$ (4) and $[Cr\{Me_4C_2(C_5H_4)\text{-}[C_5H_3B(C_6F_5)_3]\}]$ (3a): A 500 mL bulb equipped with a finger shaped extension at the bottom (OD = 23 mm, length = 70 mm) and a small magnetic stir bar was charged with **1** (0.741 g, 2.54 mmol) and $B(C_6F_5)_3$ (1.30 g, 2.54 mmol). The bulb was placed under vacuum, cooled with liquid N_2, and toluene (ca. 12 mL) was transferred into the finger under vacuum. With the toluene still frozen, the bulb was again thoroughly evacuated and closed with a Teflon-type needle valve. Upon being warmed to 35–40 °C with stirring, the reaction mixture formed a dark orange solution. Periodically the mixture was frozen by cooling the finger with liquid N_2 and the gas from the headspace was collected with a Toepler pump until no gas was further evolved. Over time, the solution turned dark green and an orange brown precipitate formed. A total of 0.49 mol gas per mol Cr was evolved and found to consist exclusively of CO by passage over a 320 °C copper oxide column to generate CO_2. The dark green solution was separated from the red-orange precipitate by filtration and the precipitate was washed with toluene (3 × 5 mL) and the washings combined with the filtrate. The precipitate was dried under vacuum, giving **4** (0.717 g, 35% yield based on **1**). $\mu_{eff} = 1.9\ \mu_B$; IR (KBr/nujol): $\tilde{\nu} = 2385$ (BH), 1989 cm^{-1} (CO); ^{1}H NMR (500.13 MHz, $[D_8]$THF, 298 K): $\delta = 3.91$ (br q, ^1J(B,H) = 85 Hz, 1H; B*H*), −1.65 ppm (br s, 12H; $(CH_3)_4C_2$); ^{11}B NMR (160.46 MHz, $[D_8]$THF, 298 K): $\delta = -22$ ppm (d, ^1J(B,H) = 85 Hz); ^{19}F NMR (282.40 MHz, $[D_8]$THF, 298 K): $\delta = -134.1$ (*o*-F), −168.6 (*p*-F), −170.7 ppm (*m*-F); elemental analysis cald (%) for $C_{35}H_{21}BCrF_{15}O$: C 52.20, H 2.63; found: C 51.23, H 2.46.

The filtrate was dried under reduced pressure and the dark green residue was washed with pentane and dried under vacuum, affording **3a** (0.977 g, 49% yield based on **1**). $\mu_{eff} = 3.9\ \mu_B$ (solid state and solution); ^{1}H NMR (300.13 MHz, C_6D_6, 298 K): $\delta = 1.12$ (br, Me), −1.80 (br, Me), −7.80 (br, Me), −10.20 ppm (br, Me); ^{19}F NMR (282.40 MHz, C_6D_6, 298 K): $\delta = -145.3$ (*p*-F), −153.4 ppm (*m*-F); ^{19}F NMR (282.40 MHz, $[D_8]$THF, 298 K): $\delta = -152.9$ (*p*-F); −159.9 ppm (*m*-F).

Characterization of reaction between 1 and $B(C_6F_5)$ at 100–105 °C—isolation of 3a and 6: A 150 mL glass vessel with a Teflon needle valve was charged with **1** (1.46 g,4.99 mmol) and $B(C_6F_5)_3$ (2.54 g, 4.96 mmol). Toluene (40 mL) was vacuum transferred into the vessel, which was cooled with liquid nitrogen. The head space was evacuated and the vessel was sealed. The mixture was thawed to room temperature, affording a clear, dark orange solution that turned somewhat darker upon being stirred overnight at room temperature. The reaction mixture was frozen and the gases in the headspace measured with a Toepler pump. Only 0.02 mol gas per mol Cr was evolved. Upon heating the reaction mixture to 100–105 °C, the solution turned dark green and gas evolution was observed. Gas was collected from the headspace periodically over 36 h until no more gas was generated. In total, 0.97 mol gas per mol Cr was collected. The reaction mixture was dried under reduced pressure and the dark green residue was washed with pentane (30 mL) and extracted with benzene (3 × 15 mL), leaving a brown-yellow solid. The combined benzene extracts were dried under reduced pressure, leaving a green solid that was washed with pentane and dried under vacuum, affording **3a** (1.81 g, 47% yield based on **1**) The brown-yellow precipitate was washed three more times with benzene and dried under vacuum to give **6** as a dark yellow powder (1.67 g, 43% yield based on **1a**). IR (KBr/nujol): $\tilde{\nu} = 2385$ cm^{-1} (BH); elemental analysis calcd for $C_{34}H_{21}BCrF_{15}$: C 53.46, H 2.50; found C 52.53, H 2.72.

Thermolysis of 4 to form $[Cr\{Me_4C_2(C_5H_4)_2\}][HB(C_6F_5)_3]$ (5) and 6: Toluene (ca. 25 mL) was transferred under vacuum to a liquid N_2 cooled, 100 mL glass vessel containing **4** (0.279 g, 0.346 mmol). With the solvent still frozen, the vessel was thoroughly evacuated and then sealed with a Teflon-type needle valve. Thawing the toluene produced a light yellow-orange solution and a suspension of solid **4**. The mixture was heated at 90–100 °C, causing the solution to turn dark green. Gases evolved by the sample were collected from the headspace periodically over 7 h until no further gas was evolved. A total of 0.98 mol gas per mol Cr was measured with the Toepler pump. Some yellow precipitate formed during the reaction. Oxidation of the gas over a heated copper oxide column revealed that it consisted entirely of CO.

The green solution was filtered to remove the yellow precipitate. Efforts to isolate the green toluene-soluble material were hampered by the tendency of the solution to form more insoluble yellow precipitate upon being concentrated under reduced pressure. Layering the toluene solution with pentane and letting it stand, undisturbed, for 2 days, yielded some dark green X-ray quality crystals along with more yellow precipitate.

Thermolysis of 4 to form 3a and 6: Toluene (5 mL) was condensed onto **4** (0.100 g, 0.129 mmol) in a 25 mL sealable glass vessel cooled with liquid N_2. The mixture was thawed and heated at 120–125 °C, causing the solution to turn green and a brownish yellow precipitate to form. After 36 h, 1.02 mol gas per mol Cr had evolved. The gas consisted of 0.68 mol CO and 0.34 mol H_2 per mol Cr. Heating the mixture for an additional 36 h at 120–125 °C yielded more brownish yellow precipitate and an additional 0.23 mol gas per mol Cr. In total, 0.90 mol CO per mol Cr and 0.35 mol H_2 per mol Cr were isolated from the reaction. The green solution was filtered from the brownish yellow precipitate, concentrated under reduced pressure and layered with pentane. After 2 days, **3a** crystallized from the mixture (28.9 mg, 28% yield). The brownish yellow pre-

cipitate of **6** was dried under vacuum to give a dark yellow powder (55 mg, 55% yield). IR (KBr/nujol): $\tilde{\nu}=2376\ cm^{-1}$ (BH).

Thermolysis of 4 under a CO atmosphere: Toluene (5 mL) was condensed into a 25 mL sealable glass vessel containing **4** (0.101 g, 0.130 mmol) cooled with liquid N_2. The mixture was thawed and an atmosphere of CO was admitted to the vessel, which was then sealed. The vessel was placed in an oil-bath (120–125 °C) and the mixture was stirred for 36 h. At the beginning an orange, almost clear solution was obtained. Later the color became slightly green and very little brownish yellow precipitate formed. When the stirring and heating were halted and the reaction mixture cooled to room temperature, the green color dissipated, and the solution turned back to orange. All gases from the vessel were collected and analyzed and found to contain only CO. No H_2 was found.

Analysis of gases generated from the thermolysis of in situ-generated [Cr(CO)H{$Me_4C(C_5H_4)[C_5H_3B(C_6F_5)_3]$}] (2) in toluene at 120–130 °C: A 100 mL sealable glass vessel was charged with **1** (0.801 g, 2.74 mmol) and $B(C_6F_5)_3$ (1.40 g, 2.74 mmol). Toluene (20 mL) was transferred under vacuum to the vessel, which was immersed in liquid N_2. With the toluene still frozen, the vessel was thoroughly evacuated and sealed. The contents were thawed, and upon warming to RT, a dark orange solution was obtained from which light orange material precipitated. The mixture was stirred overnight at RT. A dark yellowish-brown mixture was obtained. The mixture was heated with an oil-bath at 120–130 °C. Periodically the mixture was frozen in liquid N_2 and gases in the head space of the vessel were collected. After 95 h a total of 1.20 mol gas per mol Cr was collected. Analysis of the gas revealed that it consisted of 0.96 mol CO and 0.24 mol H_2 per mol Cr.

The flask contained a dark green solution and a brown-yellow precipitate, which were separated by filtration. The filtrate was dried under reduced pressure, leaving a dark green solid that was washed twice with light petroleum ether (40 mL) and dried under vacuum, affording **3a** (1.56 g, 73.7% yield).

Large-scale one-pot synthesis of 3a: A 350 mL sealable glass vessel with a magnetic stir bar was charged with **1** (3.85 g, 13.2 mmol) and $B(C_6F_5)_3$ (6.75 g, 13.2 mmol). Toluene (70 mL) was vacuum transferred to the vessel, which was cooled with liquid N_2. The head space of the vessel was evacuated thoroughly and sealed with a Teflon valve. The contents were warmed to room temperature. After stirring for 15–20 min., the mixture turned dark orange-brown and a large amount of orange crystalline solid precipitated. The precipitate is largely **2**. While the suspension was stirred overnight at room temperature, the orange precipitate disappeared and the solution turned dark brown. The solution was heated to 120–125 °C, and gases formed in the reaction were collected periodically. After 3 h the solution became dark green and a brownish-yellow precipitate formed. By 64 h, no further gas evolution was evident. A total of 1.21 mol gas per mol Cr was collected. The yellow precipitate was isolated by filtration and dried under vacuum, affording 2.06 g of **6** (20% yield based on **1**). The filtrate was dried under reduced pressure, leaving a dark green residue that was washed with pentane and dried under vacuum, affording 7.46 g of **3a** (73% yield based on **1**).

Preparation of [Cr(CO){$Me_4C_2(C_5H_4)[C_5H_3B(C_6F_5)_3]$}] (3b): A dark green solution of **3a** (346.7 mg, 0.447 mmol) in benzene (5 mL) turned brown immediately when stirred under an atmosphere of CO. The solution was layered with pentane and left at room temperature in the presence of CO. After several days, dark brown crystals had formed. The solution was decanted and the crystals were washed with pentane (10 mL) and dried under vacuum to give **3b** (291 mg, 81% yield). $\mu_{eff}=1.8\ \mu_B$ (solid and solution); IR (KBr/nujol): $\tilde{\nu}=1978\ cm^{-1}$ (CO); ^{19}F NMR (282.40 MHz, [D_8]THF, 298 K): $\delta=-158$ (*p*-F), -163 ppm (*m*-F); elemental analysis calcd (%) for $C_{35}H_{19}BCrF_{15}O$: C 52.33, H 2.38; found: C 52.46, H 2.68.

Preparation of [Cr(CNxyl){$Me_4C_2(C_5H_4)[C_5H_3B(C_6F_5)_3]$}] (3c): A dark green solution of **3a** (154.1 mg, 0.1987 mmol) in benzene (1 mL) was added to CNxyl (25.5 mg, 0.194 mmol) in a 50 mL reaction vessel. The solution immediately turned dark brown. After 6 h crystals of **3c** began to form. To stimulate additional crystallization, a few drops of petroleum ether were added occasionally to the solution. After 3 days the supernatant was decanted from the crystals, which were washed with pentane and dried in vacuum, giving **3c** (0.136 g, 71% yield). $\mu_{eff}=1.8\ \mu_B$ (solid and solution); IR (KBr/nujol): $\tilde{\nu}=2100\ cm^{-1}$ (CN); ^1H NMR (300 MHz, C_6D_6, 298 K): $\delta=8.02$ (*p*-H, xyl), 6.03 (*m*-H, xyl), 0.771 (CH_3, xyl), 4.32, 2.00, 0.771, -5.25 ppm ($C_2(CH_3)_4$); ^{13}C NMR (125 MHz, C_6D_6, 298 K): $\delta=158.4$, 142.1 (J(C,F)$=233$ Hz; $B(C_6F_5)_3$), 133.3 ppm (xyl); ^{19}F NMR (282 MHz, [D_8]THF, 298 K): $\delta=-159$ (*p*-F), -163 ppm (*m*-F); elemental analysis calcd (%) for **3c**·C_6H_6 ($C_{49}H_{34}BCrF_{15}N$): C 59.77, H 3.48, N 1.42; found: C 60.02, H 3.36, N 1.20.

Preparation of [Cr(PMe_3){$Me_4C_2(C_5H_4)[C_5H_3B(C_6F_5)_3]$}] (3d): In the glovebox, a sealable glass vessel equipped with a gas bulb was charged with **3a** (136.0 mg, 0.1754 mmol) and benzene (10 mL). All gases were thoroughly removed from the vessel on the vacuum line through a series of freeze-pump-thaw cycles. Enough PMe_3 vapor was admitted to the vacuum line to fill the gas bulb with about 2 equivalents of PMe_3 relative to **3a**. The bulb was closed from the rest the line and the PMe_3 was allowed to diffuse into the solution of **3a** overnight. Crystals of **3d** were grown by layering the solution with pentane (30 mL). After two days dark green-brown crystals of **3d** had formed. The solution was decanted from the crystals and the product was washed with pentane and dried under vacuum to give **3d** (127.7 mg, 85% yield). $\mu_{eff}=1.9\ \mu_B$ (solid and solution); ^{19}F NMR (282 MHz, [D_8]THF, 298 K): $\delta=-157$ (*p*-F), -160 ppm (*m*-F); elemental analysis calcd (%) for $C_{37}H_{28}BCrF_{15}P$: C 51.74, H 3.30; found: C 52.20, H 3.31.

Preparation of [Cr($PPhMe_2$){$Me_4C_2(C_5H_4)[C_5H_3B(C_6F_5)_3]$}] (3e): $PPhMe_2$ (77.8 mg, 0.563 mmol) was added to a solution of **3a** (205.6 mg, 0.265 mmol) in toluene (2 mL) in a 50 mL glass vessel. The clear green solution turned dark green immediately and the product precipitated. The toluene was removed under reduced pressure and the residue was redissolved in THF (1 mL). Slow diffusion of a layer of pentane into the solution afforded dark green crystals after 4 days. The crystals were isolated by filtration, washed with pentane, and dried under vacuum (yield: 156 mg, 64%). $\mu_{eff}=2.0\ \mu_B$ (solid and solution); ^{19}F NMR (282 MHz, [D_8]THF, 298 K): $\delta=-155$ (*p*-F), -159 ppm (*m*-F); elemental analysis calcd (%) for $C_{42}H_{30}BCrF_{15}P$: C 55.22, H 3.31; found: C 55.38, H 3.61.

X-ray structure determinations: Crystals of each compound were removed from the flask and covered with a layer of hydrocarbon oil. A suitable crystal was selected, attached to a glass fiber and placed in the low-temperature nitrogen stream.[49] Data for **3b** were collected using a Bruker/Siemens SMART 1 K and Siemens LT-2 A low-temperature device. Data for **3d**, **3e**, and **5** were collected at low temperature by using a Bruker APEX instrument and a Cryocool NeverIce low-temperature device. Data were measured with $Mo_{K\alpha}$ radiation, ($\lambda=0.71073$ Å) using omega scans of 0.3 ° per frame. The first 50 frames were recollected at the end of data collection to monitor for decay. Cell parameters were retrieved by using SMART[50] software and refined by using SAINTPlus[51] on all observed reflections. Data reduction and correction for Lp and decay was performed by using the SAINTPlus software. Absorption corrections were applied by using SADABS.[52] The structures were solved by direct methods and refined using the least-squares method on F^2 with the SHELXTL v. 5.10 program package.[53] Except for the disorder in **4** and **5**, all non-hydrogen atoms were refined anisotropically. In **4** the $HB(C_6F_5)_3$ goup has two positions (85:15%) and only the major component was refined anisotropically. One of perfluorophenyl rings in the major component is also disordered (40:45%). Restraints were applied to the displacement parameters and some of the B–C distances in the minor moiety. In **5** the *ansa*-chromocene backbone, a Cp ring and one perfluorophenyl ring are disordered (75:25%). Only the major disordered component was taken anisotropic. Distances and displacement parameters in the minor component were restrained. Hydrogen atoms were placed in their geometrically generated positions and refined using a riding model.

Acknowledgements

The authors are grateful to the donors of the Petroleum Research Fund, administered by the American Chemical Society, the National Science

Foundation (grant no. CHE-9816730), and the Department of Energy EPSCoR program (grant no. DE-FG0298ER45709) for their financial support. We thank Dr. Alexander Blumenfeld (University of Idaho) for his help with acquisition and interpretation of the ESR spectra. The acquisition of an ESR spectrometer by the University of Idaho was supported by the National Science Foundation and the University of Idaho Office of Research. The establishment of a single-crystal X-ray diffraction laboratory and the purchase of a 500 MHz NMR spectrometer were supported by the M. J. Murdock Charitable Trust of Vancouver, WA, National Science Foundations, and the NSF Idaho EPSCoR Program.

[1] R. P. A. Sneeden, *Organochromium Compounds*, Academic Press, New York, **1975**.
[2] R. Davis, L. A. P. Kane-Maguire, in *Comprehensive Organometallic Chemistry, Vol. 3*, (Eds.: G. Wilkinson, F. G. A. Stone, E. Abel) Pergamon, Oxford, **1982**, Chapter 26.2.
[3] K. L. T. Wong, H.-H. Brintzinger, *J. Am. Chem. Soc.* **1975**, *97*, 5143–5146.
[4] H.-H. Brintzinger, L. L. Lohr, K. L. T. Wong, *J. Am. Chem. Soc.* **1975**, *97*, 5146–5155.
[5] H. Schwemlein, L. Zsolnai, G. Huttner, H.-H. Brintzinger, *J. Organomet. Chem.* **1983**, *256*, 285–289.
[6] D. M. J. Foo, P. J. Shapiro, *Organometallics* **1995**, *14*, 4957–4959.
[7] G. J. Matare, D. M. Foo, K. M. Kane, R. Zehnder, M. Wagener, P. J. Shapiro, *Organometallics* **2000**, *19*, 1534–1539.
[8] P. J. Shapiro, R. Zehnder, D. M. Foo, P. Perrotin, P. H. M. Budzelaar, S. Leitch, B. Twamley, *Organometallics* **2006**, *25*, 719–732.
[9] P.-J. Sinnema, P. J. Shapiro, D. M. J. Foo, B. Twamley, *J. Am. Chem. Soc.* **2002**, *124*, 10996–10997.
[10] D. F. Evans, *J. Chem. Soc.* **1959**, 2003–2005.
[11] J. H. Williams, *Acc. Chem. Res.* **1993**, *26*, 593–598.
[12] G. W. Coates, A. R. Dunn, L. M. Henling, J. W. Ziller, E. B. Lobkovsky, R. H. Grubbs, *J. Am. Chem. Soc.* **1998**, *120*, 3641–3649.
[13] M. Morimoto, S. Kobatake, M. Irie, *Chem. Rec.* **2004**, *4*, 23–38.
[14] M. D. Blanchard, R. P. Hughes, T. E. Concolino, A. L. Rheingold, *Chem. Mater.* **2000**, *12*, 1604–1610.
[15] P.-J. Sinnema, J. Nairn, R. Zehnder, P. J. Shapiro, B. Twamley, A. Blumenfeld, *Chem. Commun.* **2004**, 110–111.
[16] D. M. J. Foo, P.-J. Sinnema, B. Twamley, P. J. Shapiro, *Organometallics* **2002**, *21*, 1005–1007.
[17] Efforts to trap the *ansa*-chromocene fragment with PF_3 have been unsuccessful, P. J. Shapiro, unpublished results.
[18] a) F. Köhler, W. A. Geike, *J. Organomet. Chem.* **1987**, *328*, 35–47; b) J. Blümel, M. Herker, W. Hiller, F. H. Köhler, *Organometallics* **1996**, *15*, 3474–3476; c) F. Köhler, R. de Cao, G. Manlik, *Inorg. Chim. Acta* **1984**, *91*, L1–L2; d) F. Köhler, W. Prössdorf, *Z. Naturforsch. B* **1977**, *32*, 1026–1029; e) J. Blümel, P. Hofmann, F. H. Köhler, *Magn. Reson. Chem.* **1993**, *31*, 2–6.
[19] J. A. Barrera, D. E. Wilcox, *Inorg. Chem.* **1992**, *31*, 1745–1752.
[20] D. O'Hare, V. J. Murphy, N. Kaltsoyannis, *J. Chem. Soc. Dalton Trans.* **1993**, 383–392.
[21] A. R. Okl, H. Zhang, J. A. Maguire, N. S. Hosmane, H. Ro, W. E. Hatfield, M. Moscherosch, W. Kaim, *Organometallics* **1992**, *11*, 4202–4213.
[22] V. V. Burlakov, P. Arndt, W. Baumann, A. Spannenberg, U. Rosenthal, A. V. Letov, K. A. Lyssenko, A. A. Korlyukov, L. I. Strunkina, M. Kh. Minacheva, V. B. Shur, *Organometallics* **2001**, *20*, 4072–4079.
[23] J. C. Green, C. N. Jardine, *J. Chem. Soc. Dalton Trans.* **1999**, 3767–3770.
[24] R. Choukroun, C. Lorber, B. Donnadieu, *Organometallics* **2004**, *23*, 1434–1437.
[25] J. Ruwwe, G. Erker, R. Fröhlich, *Angew. Chem.* **1996**, *108*, 108–110; *Angew. Chem. Int. Ed. Engl.* **1996**, *35*, 80–82.
[26] L. H. Dörrer, A. J. Graham, D. Haussinger, M. L. H. Green, *J. Chem. Soc. Dalton Trans.* **2000**, 813–820.
[27] V. V. Burlakov, S. I. Troyanov, A. V. Letov, L. I. Strunkina, M. K. Minacheva, G. G. Furin, U. Rosenthal, V. B. Shur, *J. Organomet. Chem.* **2000**, *598*, 243–247.
[28] S. Liu, F.-C. Liu, G. Renkes, S. G. Shore, *Organometallics* **2001**, *20*, 5717–5723.
[29] P. Perrotin, unpublished results.
[30] B. E. Carpenter, W. E. Piers, M. Parvez, G. P. A. Yap, S. J. Rettig, *Can. J. Chem.* **2001**, *79*, 857–867.
[31] $B(C_6F_5)_3$ was prepared from the reaction of C_6F_5MgBr with $BF_3(Et_2O)$ in ether. The product was purified by vacuum sublimation (120°C, 0.1 torr). See: Eur. Pat. Appl. 728760, **1996**.
[32] E. König, G. K. König, *Magnetic Properties of Coordination and Organometallic Transition Metal Compounds, Vol. 11*, Springer, Berlin, **1981**, .
[33] B. J. Burger, J. E. Bercaw, *Experimental Organometallic Chemistry*, American Chemical Society, Washington, D.C., **1985**.
[34] R. Ahlrichs, M. Bär, H.-P. Baron, R. Bauernschmitt, S. Böcker, M. Ehrig, K. Eichkorn, S. Elliott, F. Furche, F. Haase, M. Häser, C. Hättig, H. Horn, C. Huber, U. Huniar, M. Kattannek, A. Köhn, C. Kölmel, M. Kollwitz, K. May, C. Ochsenfeld, H. Öhm, A. Schäfer, U. Schneider, O. Treutler, K. Tsereteli, B. Unterreiner, M. von Arnim, F. Weigend, P. Weis, H. Weiss, Turbomole Version 5, Theoretical Chemistry Group, University of Karlsruhe, January **2002**.
[35] O. Treutler, R. Ahlrichs, *J. Chem. Phys.* **1995**, *102*, 346–354.
[36] PQS version 2.4, Parallel Quantum Solutions: Fayetteville, Arkansas (USA), **2001** (the Baker optimizer is available separately from PQS upon request).
[37] J. Baker, *J. Comput. Chem.* **1986**, *7*, 385–395.
[38] A. D. Becke, *Phys. Rev. A* **1988**, *38*, 3098–3100.
[39] J. P. Perdew, *Phys. Rev. B* **1986**, *33*, 8822–8824.
[40] K. Eichkorn, F. Weigend, O. Treutler, R. Ahlrichs, *Theor. Chem. Acc.* **1997**, *97*, 119–124.
[41] A. Schäfer, H. Horn, R. Ahlrichs, *J. Chem. Phys.* **1992**, *97*, 2571–2577.
[42] C. Lee, W. Yang, R. G. Parr, *Phys. Rev. B* **1988**, *37*, 785–789.
[43] A. D. Becke, *J. Chem. Phys.* **1993**, *98*, 1372–1377.
[44] A. D. Becke, *J. Chem. Phys.* **1993**, *98*, 5648–5652.
[45] All calculations were performed using the Turbomole functional "b3-lyp", which is not identical to the Gaussian "B3LYP" functional.
[46] A. Schäfer, C. Huber, R. Ahlrichs, *J. Chem. Phys.* **1994**, *100*, 5829–5835.
[47] A. Klamt, G. Schürmann, *J. Chem. Soc. Perkin Trans. 1* **1993**, *2*, 799–805.
[48] J. H. Jacobsen, E. Pedersen, J. Villadsen, H. Weihe, *Inorg. Chem.* **1993**, *32*, 1216–1221.
[49] H. Hope, *Prog. Inorg. Chem.* **1994**, *41*, 1–19.
[50] SMART: v.5.626, Bruker Molecular Analysis Research Tool, Bruker AXS, Madison, WI, **2002**.
[51] SAINTPlus: v. 6.45a, Data Reduction and Correction Program, Bruker AXS, Madison, WI, **2003**.
[52] SADABS: v.2.01, an empirical absorption correction program, Bruker AXS Inc., Madison, WI, **2004**.
[53] SHELXTL: v. 6.10, Structure Determination Software Suite, Sheldrick, G. M., Bruker AXS Inc., Madison, WI, **2001**.

Received: December 30, 2006
Published online: May 15, 2007

